Environmental Science & Technology

pubs.acs.org/est

Article

Microbial and Environmental Processes Shape the Link between Organic Matter Functional Traits and Composition

Ang Hu,◆ Kyoung-Soon Jang,◆ Fanfan Meng,◆ James Stegen, Andrew J. Tanentzap, Mira Choi, Jay T. Lennon, Janne Soininen, and Jianjun Wang*

Cite This: *Environ. Sci. Technol.* 2022, 56, 10504−10516

Read Online

ACCESS | Metrics & More | Article Recommendations | Supporting Information

ABSTRACT: Dissolved organic matter (DOM) is a large and complex mixture of molecules that fuels microbial metabolism and regulates biogeochemical cycles. Individual DOM molecules have unique functional traits, but how their assemblages vary deterministically under global change remains poorly understood. Here, we examine DOM and associated bacteria in 300 aquatic microcosms deployed on mountainsides that span contrasting temperatures and nutrient gradients. Based on molecular trait dimensions of reactivity and activity, we partition the DOM composition into labile-active, recalcitrant-active, recalcitrant-inactive, and labile-inactive fractions and quantify the relative influences of deterministic and stochastic processes governing the assembly of each. At both subtropical and subarctic study sites, the assembly of labile or recalcitrant molecules in active fractions is primarily governed by deterministic processes, while stochastic processes are more important for the assembly of molecules within inactive fractions. Surprisingly, the importance of deterministic selection increases with global change gradients for recalcitrant molecules in both active and inactive fractions, and this trend is paralleled by changes in the deterministic assembly of microbial communities and environmental filtering, respectively. Together, our results highlight the shift in focus from potential reactivity to realized activity and indicate that active and inactive fractions of DOM assemblages are structured by contrasting processes, and their recalcitrant components are consistently sensitive to global change. Our study partitions the DOM molecular composition across functional traits and links DOM with microbes via a shared ecological framework of assembly processes. This integrated approach opens new avenues to understand the assembly and turnover of organic carbon in a changing world.

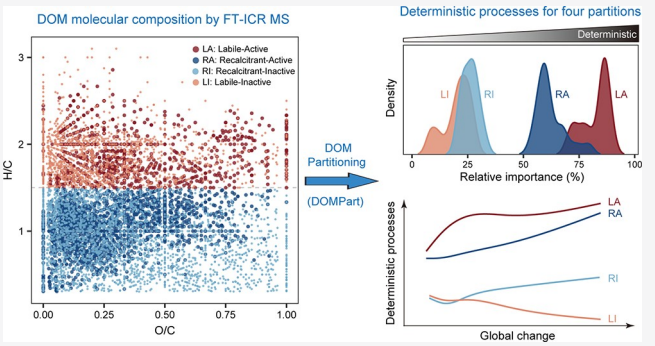

KEYWORDS: *dissolved organic matter, molecular activity, molecular reactivity, assembly processes, microbes, global change*

INTRODUCTION

Dissolved organic matter (DOM) is a complex and diverse mixture of labile and recalcitrant molecules that actively shape the biogeochemical cycles of all ecosystems on Earth.[1−6] Compared to bulk carbon pools traditionally considered, the partitioning of organic matter into various fractions, such as particulate and mineral-associated pools[7] or labile and recalcitrant pools,[8,9] is improving predictions of the vulnerability of DOM to global change. However, individual molecules vary in their sensitivity to multiple simultaneous global change drivers, such as climate change and human activities.[10,11] For instance, the decomposition of recalcitrant carbon molecules with high activation energy is more sensitive to temperature than labile carbon molecules.[10] Nutrient enrichment arising from human activities further complicates the interpretation of carbon cycling dynamics[12] because it stimulates labile carbon assimilation for microbial growth, resulting in decreased nutrients for recalcitrant carbon decomposition.[13,14] These differential sensitivities make it challenging to predict DOM turnover in a changing world. As such, there is a need to understand how the molecular composition of DOM and its dynamics respond to the synergistic effects of global drivers.

To address these challenges, we have developed a DOM partitioning framework (DOMPart) that partitions DOM molecules into four fractions based on two orthogonal trait dimensions of molecular reactivity[15−17] and activity:[18] labile-active, recalcitrant-active, recalcitrant-inactive, and labile-inactive (Figure 1a; Chart 1). Molecular reactivity is the capacity for a molecule to be degraded and thus determines the type and potential biogeochemical function of compounds. For

Received: March 1, 2022
Revised: May 19, 2022
Accepted: May 23, 2022
Published: June 23, 2022

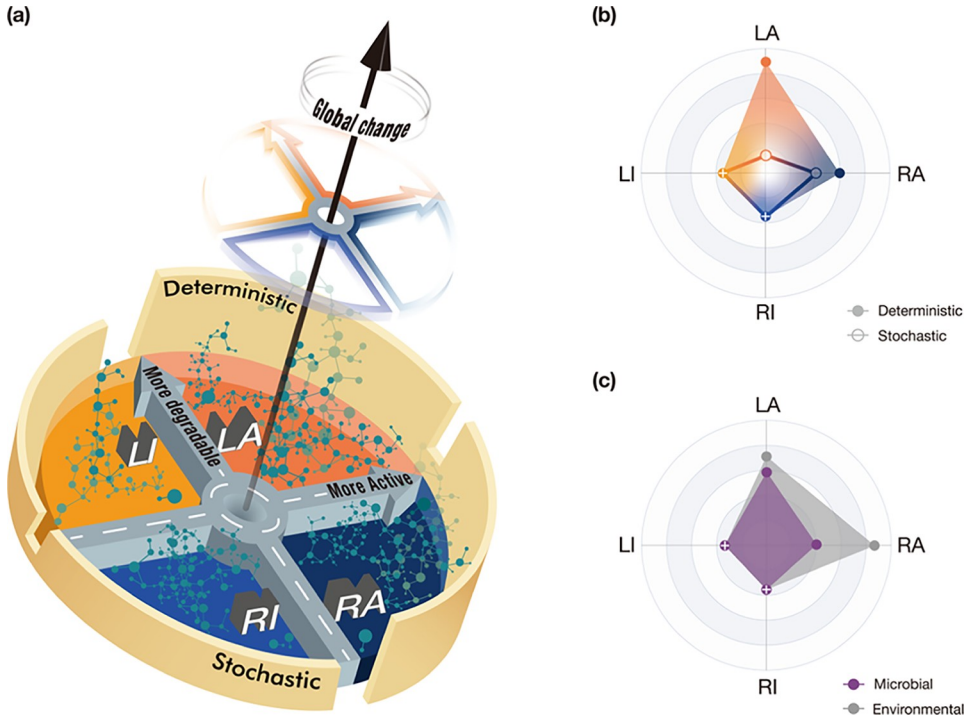

Figure 1. Framework for studying the effects of global change on dissolved organic matter (DOM) composition. (a) Conceptual framework for understanding the ecological processes under global change by including the DOM partitioning strategy. The framework displays the trade-offs in ecological processes (i.e., deterministic selection and stochastic processes) underlying four DOM fractions based on two trait dimensions of molecular reactivity and activity: labile-active (LA), recalcitrant-active (RA), recalcitrant-inactive (RI), and labile-inactive (LI) molecules. The background drawings in the four fractions are networks of molecules indicated by light green dots. The small circle in the middle indicates molecules with relatively intermediate transformations that were excluded from the four fractions. For better three-dimensional visualization, the size of the circles decreases upwards, and the arc of each quadrant circle represents the dominant ecological processes for the defined fractions under a global change scenario. More detailed hypotheses of the relative importance of ecological processes underlying the four DOM fractions are shown in panels (b) and (c). Specifically, for active fractions, the labile molecules are expected to be more deterministically assembled than the recalcitrant molecules (b). For deterministic processes, microbial communities are expected to exert more control in the labile-active fraction, whereas environmental conditions are expected to be the major determinant in the recalcitrant-active fraction (c). Dots with a cross indicate that there is no clear expectation for the relative importance of different ecological processes for the inactive fractions.

example, less biologically reactive compounds, such as recalcitrant molecules like lignin, are prone to persist in environments, whereas labile compounds like sugars are rapidly consumed by microbes.[19] In contrast, molecular activity indicates the number of potential biochemical transformations that a molecule is involved in. Activity may better relate to the rate of biochemical processes or functions than reactivity,[18] but it is not typically viewed as a molecular trait in the previous literature.

Our framework can be used to explain how changes in DOM fractions are influenced by deterministic and stochastic processes (Chart 1 Figure).[20] Identifying which, when, and where DOM assemblages are mainly governed by deterministic processes could help predict their turnover and dynamics resulting from global change. Some molecules may be selectively lost or preserved due to variation in production and transformation rates associated with specific environmental conditions and biotic interactions. These are considered deterministic processes, a perspective that is analogous to the deterministic assembly of ecological communities arising from birth and death events (Chart 1 Figure). Deterministic processes can lead to a pattern of divergent molecular composition across local assemblages via "variable selection" or convergent molecular composition via "homogeneous selection".[21,22] Variable selection involves molecules being filtered in different ways by a shift in environmental conditions, whereas homogeneous selection involves local environments consistently selecting for the same types of molecules.[22] Similarly, molecular assemblages can be influenced by stochastic processes analogous to those comprising ecological neutral theory such as drift and dispersal (Chart 1 Figure).[23] For example, stochastic processes may be important when fewer molecules are produced or transformed, consistent with ecological and evolutionary expectations that random events are influential for small-sized populations. Compared to stochastic processes, deterministic processes are jointly influenced by biotic and environmental variables, as well as intrinsic traits of DOM, which could ultimately result in predictable changes in molecular composition in response to environmental changes. Variation in the influence of these deterministic processes would, therefore, imply the sensitivity of compositional turnover of DOM to global change.

Here, we examine how the ecological mechanisms structuring DOM assemblages vary along global change gradients using 300 aquatic microcosms enriched with varying nutrient levels deployed on subtropical and subarctic mountainsides in China and Norway.[24,25] This experiment is characterized by identical initial DOM supply and composition but different locally colonized microbial communities,[24] which allowed us to compare compositional dynamics of DOM across temperature and nutrient gradients under field conditions. The two global change drivers jointly generated

https://doi.org/10.1021/acs.est.2c01432
Environ. Sci. Technol. 2022, 56, 10504−10516

Chart 1. Glossary of Terms for Merging Organic Chemistry and Ecology

Chart 1 |

Molecular Reactivity. Molecular reactivity is the capacity for a reaction of dissolved organic matter, which is constrained by molecular compounds or functional groups, and reflects the bioavailability and vulnerability to degradation (i.e., the degree of recalcitrance or lability). It is quantified with metrics such as H/C ratio, aromaticity index, and double bond equivalents.

Molecular Activity. Molecular activity is the performance of a reaction involving the modification of dissolved organic matter. It is quantified as the number of putative molecular transformations, i.e., the gain or loss of molecular groups between two DOM molecules. Gains and losses are quantified by mapping mass differences in pairwise m/z peak comparisons to a database of known mass differences transferred in common biochemical transformations (e.g., glucose and amines). Molecular transformations could relate to the rate of biochemical processes (or functions) and thus be used to distinguish the relatively active from inactive molecules.

Labile Fraction. Labile fraction is the category of reactivity that includes DOM molecules with a H/C ratio of ≥1.5; it is considered more bioavailable and less resistant to degradation.

Recalcitrant Fraction. Recalcitrant fraction is the category of reactivity that includes DOM molecules with a H/C ratio of <1.5; it is considered less bioavailable and more resistant to degradation.

Active Fraction. Active fraction is the category of activity including molecules involved in numerous (e.g., >10) molecular transformations.

Inactive Fraction. Inactive fraction is the category of activity including molecules involved in a few (e.g., ≤1) molecular transformations.

DOM Partitioning. DOM partitioning is the process of categorizing DOM molecules based on their molecular reactivity and activity: labile-active, recalcitrant-active, recalcitrant-inactive, and labile-inactive molecules (Figure 1a). It should be noted that the number of transformations a molecule is involved in represents a continuum of activity, and molecules with a relatively intermediate number of transformations (e.g., between 2 and 10) are excluded from the defined active and inactive fractions. Further development of the DOM partitioning framework could be used to include molecules with intermediate activity.

Energy Supply. Energy is supplied to aquatic ecosystems in the form of organic carbon, which can be used as an electron donor for chemoorganotrophic metabolism of diverse microbial populations. Organic carbon is derived from multiple sources including terrestrial vegetation and phytoplankton. The energy supply could be influenced by a combination of global change drivers such as elevated temperature and nutrient enrichment.

Ecological Processes. The processes that influence the composition of DOM are analogous to the ecological processes that control the assembly of biological communities. The processes include five components: variable selection, homogeneous selection, homogenizing dispersal, dispersal limitation, and drift. We considered selection-based assembly to be deterministic processes, while dispersal and drift were treated as stochastic processes (see Box 1 Figure).

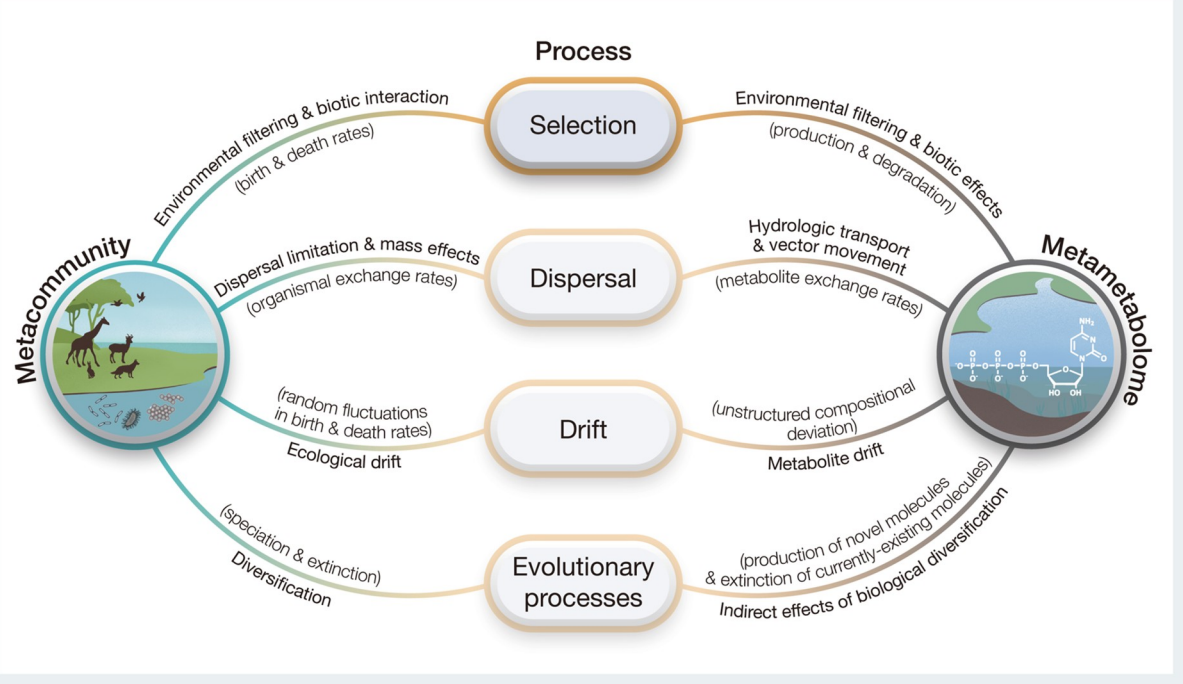

Chart 1Figure: Ecological processes underlying DOM assemblages (i.e., metabolome) analogous to ecological communities (i.e., metacommunities) and their transferable principles related to DOM organization. DOM can be assembled through selection, dispersal, drift, and evolutionary processes. These processes result in the production and/or degradation of DOM molecules (i.e., metabolites), which are akin to birth and/or death of organisms, respectively. Metabolite drift can be indirectly driven by ecological drift in microbial communities. More details are discussed in the main text.

https://doi.org/10.1021/acs.est.2c01432
Environ. Sci. Technol. 2022, 56, 10504−10516

an energy supply gradient, which was reflected by the primary productivity of algae (Figure S1). Briefly, we selected five different elevations on each mountainside, and at each elevation, we established 30 microcosms composed of natural lake sediments and artificial lake water with 10 nutrient levels ranging from 0 to 36 mg N L^{-1}. The sediment bacteria were examined using high-throughput sequencing of 16S rRNA genes.[24] Additionally, the sediment DOM was examined using ultra-high-resolution electrospray ionization Fourier transform ion cyclotron resonance mass spectrometry (FT-ICR MS).[25]

We evaluated the hypotheses that the four DOM fractions are governed by different ecological processes and that their relative importance will be modified by the joint influence of temperature and nutrient concentrations (Figure 1). More specifically, for a given global change scenario, we predicted that both active and labile DOM fractions would be primarily governed by deterministic processes[20] associated with microbial interactions (Figure 1b,c) because microbes have a high substrate specificity and preferentially consume nutrient-rich substrates to support biosynthetic processes.[26−28] Under a future global change scenario such as elevated temperature and nutrient concentrations, the relative importance of deterministic processes is expected to vary unpredictably across DOM fractions. This is because the responses of recalcitrant molecules to environmental and microbial processes could be greater than,[29] equivalent to,[8] or even less than[30] those of the labile molecules, whereas a few studies document the responses of inactive fractions. Our results now show that the active and inactive fractions of DOM assemblages are structured by contrasting ecological processes, and their recalcitrant components are unexpectedly sensitive to future global change. The integration of the DOMPart framework into the fundamental mechanisms controlling the molecular composition of DOM could improve our understanding of the functional properties of organic carbon and its dynamics under global change.

MATERIALS AND METHODS

Experimental Design. To examine biotic (i.e., microbial) vs abiotic effects on contrasting DOM fractions, we conducted field experiments along mountainsides in China and Norway. We took advantage of elevational temperature gradients as natural experiments to understand the responses of biological communities and ecosystem function to global change.[31] The comparative field microcosm experiments were conducted in a subtropical region, Laojun Mountain in China (26.6959 N; 99.7759 E), and in a subarctic region, Balggesvarri Mountain in Norway (69.3809 N; 20.3483 E), in September−October and July 2013, respectively, as first reported in Wang et al. (2016).[24]

On each mountainside, we selected five different elevations. The elevations were 3822, 3505, 2915, 2580, and 2286 m a.s.l. on Laojun Mountain in China and 750, 550, 350, 170, and 20 m a.s.l. on Balggesvarri Mountain in Norway. At each elevation, we established 30 aquatic microcosms (1.5 L bottle) composed of 15 g of sterilized lake sediments and 1.2 L of sterilized artificial lake water. The addition of 15 g of sterilized sediments at the bottom of bottles formed an ∼5 mm sediment layer to create a diffusive boundary layer at the sediment−water interface. We then added nutrients to the overlying water in each bottle at 1 of 10 levels of 0, 0.45, 1.80, 4.05, 7.65, 11.25, 15.75, 21.60, 28.80, or 36.00 mg N L^{-1} of KNO_3. To compensate for nitrate additions shifting stoichiometric ratios, KH_2PO_4 was added to the bottles so that the N/P ratio of the initial overlying water was 14.93, which was similar to the annual average ratio in Taihu Lake in 2007 (i.e., 14.49). We used the term "nutrient enrichment" to refer to manipulations of both nitrate and phosphate, the former of which was used to represent nutrient enrichment in the statistical analyses due to the consistent N/P ratio. Each nutrient level was replicated three times. The employed nutrient gradient was extensive enough to mimic the conditions ranging from high latitude and high elevation lakes in Norway to more eutrophic lakes in subtropical China, which enables us to reach general conclusions across contrasting climate zones. The bottles were buried into the local soils by 10% of their height to buffer against large air temperature variations.

All microcosms being simple had the same initial sediment and water conditions, and we only altered nutrients and temperature (here elevation). The lake sediments were obtained from the center of Taihu Lake, China, and were aseptically canned per bottle after autoclaving. The sterilized sediments were considered a standardized "culture medium" for microbial colonization and can theoretically be produced from any lake. This is the key to enabling us to quantitatively examine biotic (i.e., microbial) vs abiotic effects on contrasting DOM fractions. The colonized communities in the microcosms allowed us to capture the local and regional species pools at each experimental site. Such a field experiment across climate zones enables us to maximize the variations in microbial community composition among the 300 microcosms. At the start of the experiment, bacterial biomass was low, while the sediment bacterial species were gradually and continuously selected by dispersal processes and by environmental filters of the overlying water and sediments and were expected to form stable and adaptive communities after a 1 month incubation. The simplified experimental ecosystems were highly ideal and useful for examining the ecological processes underlying DOM assemblages in response to global change drivers.

Sample Collection and Biogeochemical Analyses. At the end of the 1 month experimental period, we aseptically sampled the overlying water and sediments of the 300 bottles (i.e., 2 mountains × 5 elevations × 10 nutrient levels × 3 replicates) for the following analyses of environmental variables, bacterial, DOM compositions. Details on field experiments, sample collection, environmental variables, bacterial, and DOM analyses were described in Wang et al. (2016)[24] and Hu et al. (2021).[25] Briefly, environmental variables were measured for each sediment and water sample (Table S1), including energy supply (i.e., water pH, sediment chlorophyll *a*, sediment total organic carbon, and dissolved organic carbon), and contemporary nutrients (i.e., total nitrogen, total phosphorus, NO_x^-, NO_2^-, NH_4^+, and PO_4^{3-} in the sediments and NO_3^-, NO_2^-, NH_4^+, and PO_4^{3-} in the overlying water). Sediment bacteria were examined using high-throughput sequencing of 16S rRNA genes. The sequences were processed in QIIME (v1.9),[32] and operational taxonomic units (OTUs) were defined at a 97% sequence similarity. The bacterial sequences were rarefied to 20,000 per sample.

Highly accurate mass measurements of DOM within the sediment samples were conducted using a solariX XR 15T ultra-high-resolution Fourier transform ion cyclotron resonance mass spectrometer (FT-ICR MS, Bruker Daltonics, Billerica, MA). The FT-ICR MS was coupled to an electrospray ionization (ESI) interface, as demonstrated

https://doi.org/10.1021/acs.est.2c01432
Environ. Sci. Technol. 2022, 56, 10504−10516

previously[33] with some modifications. DOM was solid-phase-extracted for the FT-ICR MS measurement[34] with some modifications. Data analysis software (BrukerDaltonik version 4.2) was used to convert raw spectra to a list of m/z values using an FT-MS peak picker with a signal-to-noise ratio (S/N) threshold set to 7 and absolute intensity threshold to a default value of 100. Putative chemical formulae were assigned using an in-house software Formularity[35] following the compound identification algorithm.[36] The assigned molecules were categorized into eight tentative compound classes based on van Krevelen diagrams:[37] lipids (O/C = 0−0.3, H/C = 1.5−2.0), proteins (O/C = 0.3−0.55, H/C = 1.5−2.2), amino sugars (O/C = 0.55−0.67, H/C = 1.5−2.2), carbohydrates (Carb; O/C = 0.67−1.2, H/C = 1.5−2), unsaturated hydrocarbons (UnsatHC; O/C = 0−0.1, H/C = 0.7−1.5), lignin (O/C = 0.1−0.67, H/C = 0.7−1.5), tannin (O/C = 0.67−1.2, H/C = 0.5−1.5), and condensed aromatics (ConHC; O/C = 0−0.67, H/C = 0.2−0.7). More details on bacterial community and DOM analyses are provided in the Supplementary Methods.

DOM Features. The relative abundance of molecules was calculated by the normalization of signal intensities of assigned peaks to the sum of all intensities within each sample. The chemical characteristics of molecules were evaluated by 16 molecular traits related to molecular weight, stoichiometry, chemical structure, and oxidation state (Table S1). These traits were mass, the number of carbon (C), the modified aromaticity index (AI_{Mod}),[12,38] double bond equivalents (DBEs),[38] DBE minus oxygen (DBE_O),[38] DBE minus AI (DBE_{AI}),[38] standard Gibb's free energy of carbon oxidation (GFE),[39] Kendrick defect ($kdefect_{CH2}$),[40] nominal oxidation state of carbon (NOSC),[38] O/C ratio, H/C ratio, N/C ratio, P/C ratio, S/C ratio, and carbon use efficiency (Y_{met}).[41] These traits were calculated for each molecule using the R package ftmsRanalysis[42] and scripts at https://github.com/danczakre/ICRTutorial. DBE represents the number of unsaturated bonds and rings in a molecule.[38] Higher values of DBE, AI, and NOSC all indicate a higher recalcitrance of DOM. A large Kendrick defect can indicate a higher degree of oxidation. Lower values of Y_{met} indicate a higher thermodynamic efficiency of metabolic reactions involved in biomass production.[41] Weighted means of formula-based molecular traits (e.g., the $Mass_{wm}$ for Mass) were calculated as the sum of the trait of the individual molecule ($Mass_i$) and relative intensity I_i divided by the sum of all intensities ($Mass_{wm} = \Sigma(Mass_i \times I_i)/\Sigma(I_i)$) using the R package FD V1.0.12.[43]

The potential biochemical transformations of molecules were identified following the previous literature.[2,18,44] All possible pairwise mass differences between FT-ICR MS peaks were compared with a database of 1255 commonly observed mass differences associated with biochemical transformations. For example, a mass difference of 18.03437 corresponds to a loss or gain of an ammonium group, while a difference of 180.06339 would putatively indicate loss or gain of a glucose molecule. Inferring biochemical transformations is possible due to the ultrahigh mass resolution of FT-ICR MS data. Transformations were then counted for each molecule to classify molecular activity. The database and the scripts for the calculation of biochemical transformations are publicly available at https://github.com/danczakre/Meta-Metabolome_Ecology.

Putative interactions between molecules were quantified using co-occurrence network analysis. The co-occurrence network was inferred based on the SparCC (Sparse Correlations for Compositional data)[45] correlation matrix constructed with the R package SpiecEasi V1.0.7.[46] Molecules observed in more than 1/3 of the total samples in China or Norway were retained for correlation calculations. The threshold value of SparCC ρ correlations for generating co-occurrence networks was 0.30 to filter the uncorrelated or weakly correlated interactions. We then calculated network properties, including the degree and betweenness centrality, for each node (i.e., molecule) with the R package igraph V1.2.6. Degree is defined as the number of edges that connects a focal node to other nodes.[47] Molecules with a higher degree are more interconnected within an assemblage. Betweenness centrality measures the extent to which a node lies on paths between other nodes. Molecules with a higher betweenness centrality communicate more with other molecules within an assemblage.[47] Network images were generated with Gephi (http://gephi.github.io/).

Partitioning DOM. We parsed DOM assemblages of 19,538 molecular formulae into four contrasting partitions by considering two molecular trait dimensions: reactivity and activity. Reactivity represents the potential utilization of organic compounds by microorganisms and generally consists of the lability and recalcitrance,[16] which could be, respectively, differentiated by values above and below a H/C ratio of 1.5.[37,48] According to D'Andrilli et al. (2015), the cutoff of H/C ratio = 1.5 is the threshold of molecular lability vs recalcitrance. This cutoff was developed from the FT-ICR MS molecular data and can be visualized in van Krevelen diagrams. For the activity, DOM comprises biochemically active and inactive fractions based on the number of potential molecular (or metabolite) transformations in biochemical processes.[18] Transformations were counted for each molecule, and we assumed that molecules involved in less than 1 and more than 10 transformations were considered "inactive" and "active", respectively. The selection of a transformation cutoff may not be generalizable across studies but serves to demonstrate the potential utility of our DOMPart framework. The cutoff of 10 transformations was based on two observations. First, there was a clear decrease in the number of transformations above 10 but still sufficient number of active molecules in each window for the moving-window analyses and βNTI null models (Figure S2). Second, the results of assembly processes for molecules with transformations from 2 to 10 were similar to those with ≤1 but differed greatly for those >10 transformations (Figure S3). The cutoff of 1 transformation was largely based on a few transformations and sufficient numbers of inactive molecules in each window for the statistical analyses. Thus, to focus on the main messages in this study, we only showed results regarding transformations ≤1 and >10 to represent "inactive" and "active" fractions, respectively. Overall, we had four molecular reactivities × activity combinations: labile-active (H/C ≥ 1.5, transformations > 10), recalcitrant-active (H/C < 1.5, transformations > 10), recalcitrant-inactive (H/C < 1.5, transformations ≤ 1), and labile-inactive (H/C ≥ 1.5, transformations 1.5).

Statistical Analyses. We disentangled the ecological processes structuring the four DOM fractions identified by the DOMPart framework from three perspectives.

First, we quantified the relative importance of stochastic versus deterministic processes for the assembly of organic molecules into the DOM pools. We used an ecological null modeling approach,[20] which involves the construction of a

https://doi.org/10.1021/acs.est.2c01432
Environ. Sci. Technol. 2022, 56, 10504−10516

dendrogram built from the functional traits of DOM molecules. This approach is analogous to functional trait similarities in ecological analyses.[49,50] Specifically, we generated a molecular characteristic dendrogram using 16 molecular traits (Table S1).[20] We calculated the potential molecular similarities between chemical formulae using Euclidean distances, which were then used to perform a UPGMA hierarchical cluster analysis using the "average" method with the function "hclust" in the R package stats V3.6.1. We then quantified the molecule dendrogram-based turnover in molecular composition between a given pair of assemblages using the β-mean nearest taxon distance metric (βMNTD).[20] βMNTD estimates the mean dendrogram distance to the closest relative in a paired assemblage for all molecules

$$\beta\text{MNTD} = \frac{\sum_{i_k=1}^{n_k} f_{i_k} \min(d_{i_k j_m}) + \sum_{i_m=1}^{n_m} f_{i_m} \min(d_{i_m j_k})}{2}$$

where f_{i_k} is the relative abundance of molecule i in assemblage k, n_k is the number of molecules in assemblage k, and $\min(d_{i_k j_m})$ is the minimum dendrogram distance between molecule i in assemblage k and molecule j in assemblage m.

β-diversity null modeling was performed to examine whether molecular assemblages were significantly more or less similar than would be expected by random chance alone and to assess whether assemblages were deterministically or stochastically assembled. We thus calculated the dendrogram-based β-nearest taxon index (βNTI), which compares the observed β-mean nearest taxon distance (βMNTD) between pairs of samples to a null expectation generated by breaking observed dendrogram associations[20]

$$\beta\text{NTI} = -1\left(\frac{\beta\text{MNTD}_{\text{obs}} - \overline{\beta\text{MNTD}_{\text{null}}}}{\beta\text{MNTD}_{\text{sd}}}\right)$$

where $\beta\text{MNTD}_{\text{obs}}$ is the observed βMNTD for the observed assemblages, $\overline{\beta\text{MNTD}_{\text{null}}}$ is the mean βMNTD for the null assemblages, and $\beta\text{MNTD}_{\text{sd}}$ is the standard deviation of $\beta\text{MNTD}_{\text{null}}$ values. For βNTI calculations, 999 randomized null assemblages were generated by shuffling the tips of dendrogram and βNTI was calculated using the "qpen" function (ab.weight = FALSE) in the R package iCAMP V1.2.8.[51] As such, peak intensities could not contain the same ecological meaning as variation in species abundances. The use of peak intensities from FT-ICS MS is therefore not suitable for null modeling without additional information linking peak intensities to concentrations. Analogous to applying this metric to ecological communities,[52,53] the degree of tip-level clustering or overdispersion in metabolite assemblages can be quantified. Deterministic processes explain the observed assemblage differences if a $|\beta\text{NTI}|$ value is greater than 2, while stochastic processes are responsible for assemblage differences if a $|\beta\text{NTI}|$ value is less than 2. Deterministic processes could be further broken down into variable selection if βNTI is greater than 2, and homogeneous selection if βNTI is less than -2.

Second, for deterministic processes, the relative contributions of bacterial communities and environmental variables were quantified for the assemblages of DOM partitions with variation partitioning analysis (VPA).[54] We used individual bacterial genera to perform a principal coordinate analysis (PCA), and the first seven axes of PCA accounting for 90.6% of the total variance were used as explanatory variables representing the bacterial communities. Environmental variables included chlorophyll *a*, total organic carbon, dissolved organic carbon, total nitrogen, total phosphorus, NO_x^-, NO_2^-, NH_4^+, and PO_4^{3-} in the sediments and pH, NO_3^-, NO_2^-, NH_4^+, and PO_4^{3-} in the overlying water (Table S1). We selected the above explanatory variables for regression analyses by forward selection.[55] VPA was performed with the R package vegan V2.4.6.[54]

Third, to study further potential drivers of variation in DOM assembly processes, we used the synthetic variable of energy supply to represent the joint outcome of increasing temperature and nutrient enrichment that characterize global change. We used water pH as an easily measured *in situ* proxy for energy supply, as opposed to laboratory-based measurements that were more removed from the field system. The link between energy supply and joint influences of temperature and nutrients was supported by these variables being positively associated with primary productivity, which was further correlated with water pH (R^2 = 0.60, P < 0.05; Figure S1 and Table S2). That is, water pH could represent primary productivity due to its strong positive correlation with sediment chlorophyll *a* at almost all nutrient levels and elevations due to depleting dissolved CO_2 upon algae growth.[24] In addition, we observed no predictable patterns in the relative influences of ecological processes on DOM assembly along either global change driver (Figures S4 and S5), but water pH often showed the highest correlations with βNTI across DOM fractions with some exceptions (Figures S6 and S7). This result indicates that the integrated supply of kinetic (i.e., temperature) and potential (i.e., nutrients) energies is more important in driving molecular composition than either type of energy on its own.

To assess the effect of increasing energy supply on the ecological processes underlying DOM partitions, we used a moving-window approach.[56,57] This approach enables continuous and/or sharp transitions in ecological processes to be identified along a continuum of global change drivers. We first sorted the samples along the energy supply gradient, from minimum to maximum water pH, separately for China and Norway. We used 1/3 of samples (i.e., 50) as the window size, generating 101 windows (e.g., 1−50, 2−51, ..., 101−150 consecutive samples). We then calculated the mean pH for each window, resulting in a pH gradient ranging from 8.0 to 10.2 in China (gradient across individual samples from 7.5 to 10.8) and a gradient from 7.6 to 9.1 in Norway (full gradient from 7.4 to 10.0) (Figures S8 and S9). For each window, we performed analyses of the βNTI null modeling and VPA. To examine the variability of ecological processes along the energy supply gradient, we calculated the ratio of standardized deviation and mean of the relative importance of each ecological process (i.e., variable selection, homogeneous selection, or stochastic processes) by randomly using 50, 60, 70, or 80 windows (100 bootstraps) along the energy supply gradient for each DOM partition in China or Norway. Additionally, we confirmed that the results were robust to window size by repeating the analyses with a fixed size of 60 samples (Figure S10).

RESULTS AND DISCUSSION

Chemical Characteristics of the Four DOM Fractions. In total, 19,538 molecules in the 300 microcosms were parsed into four fractions based on their reactivity and activity: labile-

https://doi.org/10.1021/acs.est.2c01432
Environ. Sci. Technol. 2022, 56, 10504−10516

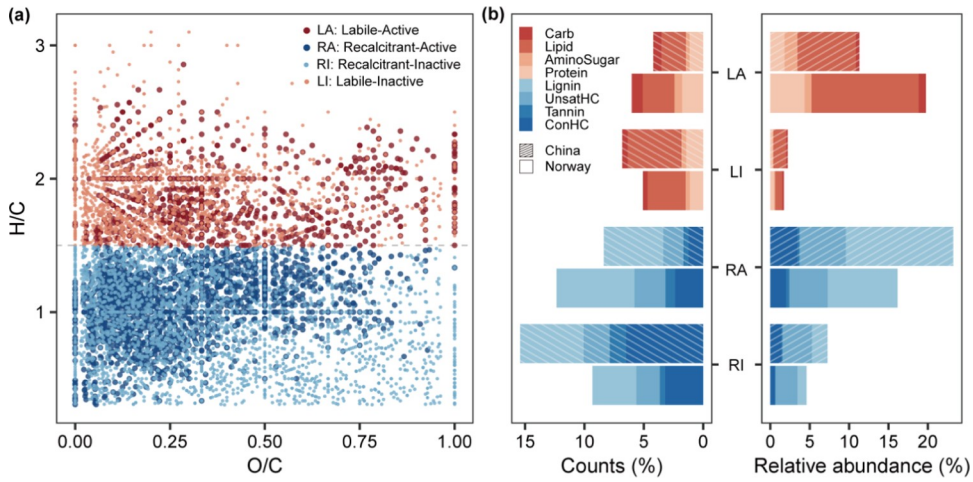

Figure 2. Molecular composition of dissolved organic matter (DOM) in China and Norway. (a) Van Krevelen diagrams showing the distribution of the molecules in the four partitioned fractions: labile-active (LA), recalcitrant-active (RA), recalcitrant-inactive (RI), and labile-inactive (LI) molecules. There was a large overlap in the van Krevelen space between active and inactive molecules, represented by large and small dots, respectively, which, however, highlights the importance of including activity as a second dimension of traits. (b) The relative abundance of DOM categories of compound classes in China and Norway. The different colors from red to gray represent differences in degradability from lability to recalcitrance.

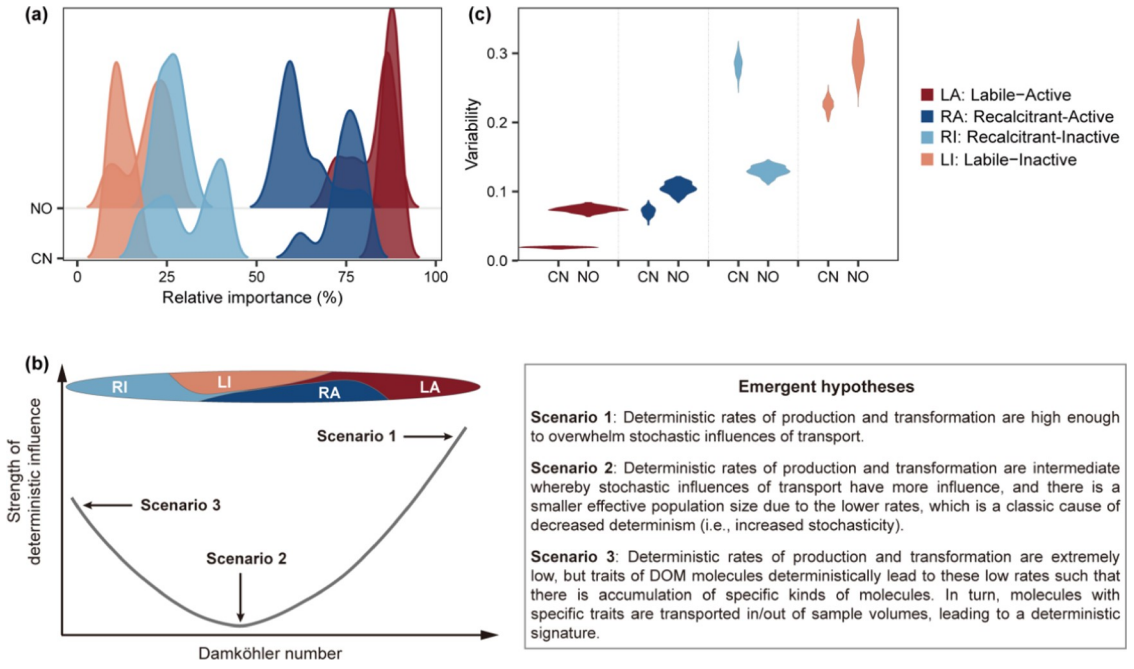

Figure 3. Ecological processes structuring dissolved organic matter (DOM) fractions under global change. (a) The distribution of the relative importance of variable selection for four DOM fractions in China (CN) and Norway (NO). The other ecological processes, that is, homogeneous selection and stochastic processes, are shown in Figure S14. The four DOM fractions are labile-active (LA), recalcitrant-active (RA), recalcitrant-inactive (RI), and labile-inactive (LI) based on two dimensions of molecular reactivity and activity. (b) Emergent hypotheses to explain ecological processes structuring the dynamics of DOM compositional change. The four DOM fractions can be transported into and out of a given sample volume in which production and transformation occur. The combined rate of production and transformation relative to the rate of transport is analogous to the Damköhler number. The labile-active and recalcitrant-inactive fractions are hypothesized to have the highest and lowest Damköhler numbers, respectively. We further propose that the relative influences of stochastic and deterministic processes over the DOM assembly are related to the Damköhler number, though the relationship is not monotonic, but instead has a concave functional form for reasons summarized in the figure panel. A DOM pool, indicated by the ellipse, could be partitioned into the four fractions along the Damköhler number gradient. In the ellipse, the four fractions are putatively distributed along the Damköhler number gradient. RI and LA will have the lowest and highest Damköhler numbers, respectively. LI and RA will occur at intermediate positions along the gradient. Effective population size indicates the number of molecules that are actively associated with production and transformation. (c) Violin plots of the variability of the relative importance of variable selection for four DOM fractions in China and Norway. Variability was calculated as the ratio of the standardized deviation to mean of the relative importance of each ecological process calculated across the pH gradients.

https://doi.org/10.1021/acs.est.2c01432
Environ. Sci. Technol. 2022, 56, 10504−10516

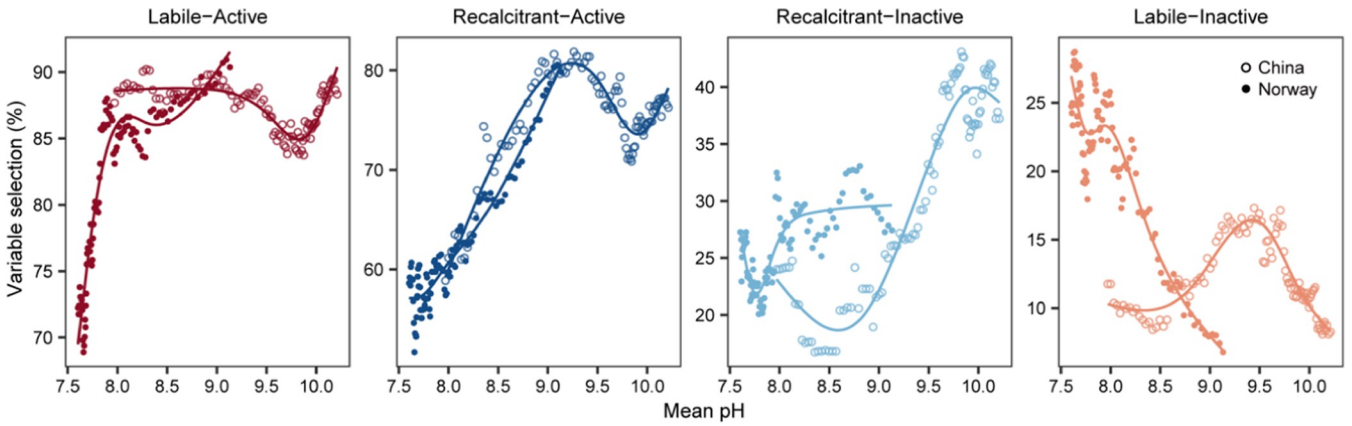

Figure 4. Effects of energy supply on the relative importance of ecological processes structuring dissolved organic matter (DOM) fractions. We plotted the relative importance of variable selection against pH for four DOM fractions in China (hollow points) and Norway (solid points). The other ecological processes, that is, homogeneous selection and stochastic processes, are shown in Figure S17. Relationships are visualized with generalized additive models with a k of 5. The four DOM fractions are labile-active, recalcitrant-active, recalcitrant-inactive, and labile-inactive molecules and were based on two dimensions of molecular reactivity and activity.

active, recalcitrant-active, recalcitrant-inactive, and labile-inactive molecules (Figures 1a and 2a and Table S3). We found that molecular activity could provide complementary information to molecular reactivity, which is supported by the overall overlapped positions in the van Krevelen space between active and inactive molecules with a H/C ratio above or below 1.5 (Figure 2a). As expected, there were distinct molecular characteristics among the four fractions in both study regions. Specifically, there were clear differences in the relative abundance of molecular compounds between active and inactive fractions for both labile and recalcitrant molecules (Figure 2b). Compared to active fractions, there were relatively more inactive molecules (15−23% of all molecules; Table S3), but this fraction had lower relative abundances (7−10%, on average; Figure S11) and fewer molecular interactions, as indicated by a lower degree and betweenness centrality in co-occurrence networks constructed for the DOM assemblages (Figure S12). Recalcitrant fractions, particularly the recalcitrant-inactive molecules, had the highest mass and recalcitrance, the latter of which was indicated by molecular traits such as a low H/C ratio and high values for the aromaticity index, double bond equivalents, and nominal oxidation state of carbon[12] (Figure S13).

Variation of Ecological Processes across the Four Fractions. The mechanisms underlying molecular assemblages of the four DOM fractions were examined with dendrogram-based null modeling.[20] We found that the molecular assemblages were jointly structured by deterministic and stochastic processes, and their relative importance varied across DOM fractions (Figures 3a, S14, and S15). Specifically, deterministic processes leading to variable selection dominated the labile-active fraction with a mean relative importance of 87 and 82% in China and Norway, respectively. Variable selection was much less important in recalcitrant-active (75 and 62%), recalcitrant-inactive (31 and 26%), and labile-inactive fractions (12 and 20%) (Figure 3a). The variation in assembly processes across DOM fractions indicates that, independent of the traditionally considered molecular reactivity or bioavailability (i.e., lability vs recalcitrance),[9,58,59] deterministic and stochastic processes primarily structured active and inactive fractions of DOM, respectively. We also found that there were contrasting patterns in ecological processes underlying both labile and recalcitrant fractions for active versus inactive molecules. For active molecules, the recalcitrant fraction was more stochastic than the labile fraction, which is consistent with our initial hypothesis (Figure 1b). Unexpectedly, however, inactive molecules showed the opposite pattern, whereby the recalcitrant fraction was more deterministic than the labile fraction (Figure 3a).

Large variation in the relative importance of deterministic processes across DOM fractions as observed here has not been reported previously. However, we offer some potential explanations for these results. We suggest that variation in the influence of deterministic processes may be associated with differences in ecosystem properties that influence organic carbon persistence.[60,61] For example, variation in physico-chemical factors such as redox conditions and mineral sorption, and biological effects caused by extracellular enzyme diffusion, can impose different constraints on the decomposition of DOM fractions. Spatial and/or temporal variation in these factors may, in turn, lead to variation in the influences of deterministic processes. If each factor selects for different types of DOM, their influences may further interact and modify signals of deterministic processes.

Alternatively, variation in the influence of deterministic processes could be tied to different rates of production and transformation of the DOM fractions. For instance, stronger influences of deterministic processes in the active fraction could be due to shorter time scales of DOM production and transformation, relative to the inactive fraction. Rapid rates that vary systematically across molecules based on molecular traits should, in theory, lead to stronger influences of deterministic processes; for example, if certain types of molecules are selected for or against based on variation in production and transformation rates. In contrast, the putatively low rates of production and transformation of the inactive fraction may allow for greater stochasticity, potentially due to larger influences of spatial movement of molecules effectively diluting otherwise deterministic outcomes. This is conceptually analogous to the Damköhler number, which is often used in hydrology and biogeochemistry to quantify the influence of reaction rate relative to the rate of solute transport.[62,63] That is, for the inactive fraction, the rate of DOM transport into or out of a given sample volume may have a larger influence over

https://doi.org/10.1021/acs.est.2c01432
Environ. Sci. Technol. 2022, 56, 10504−10516

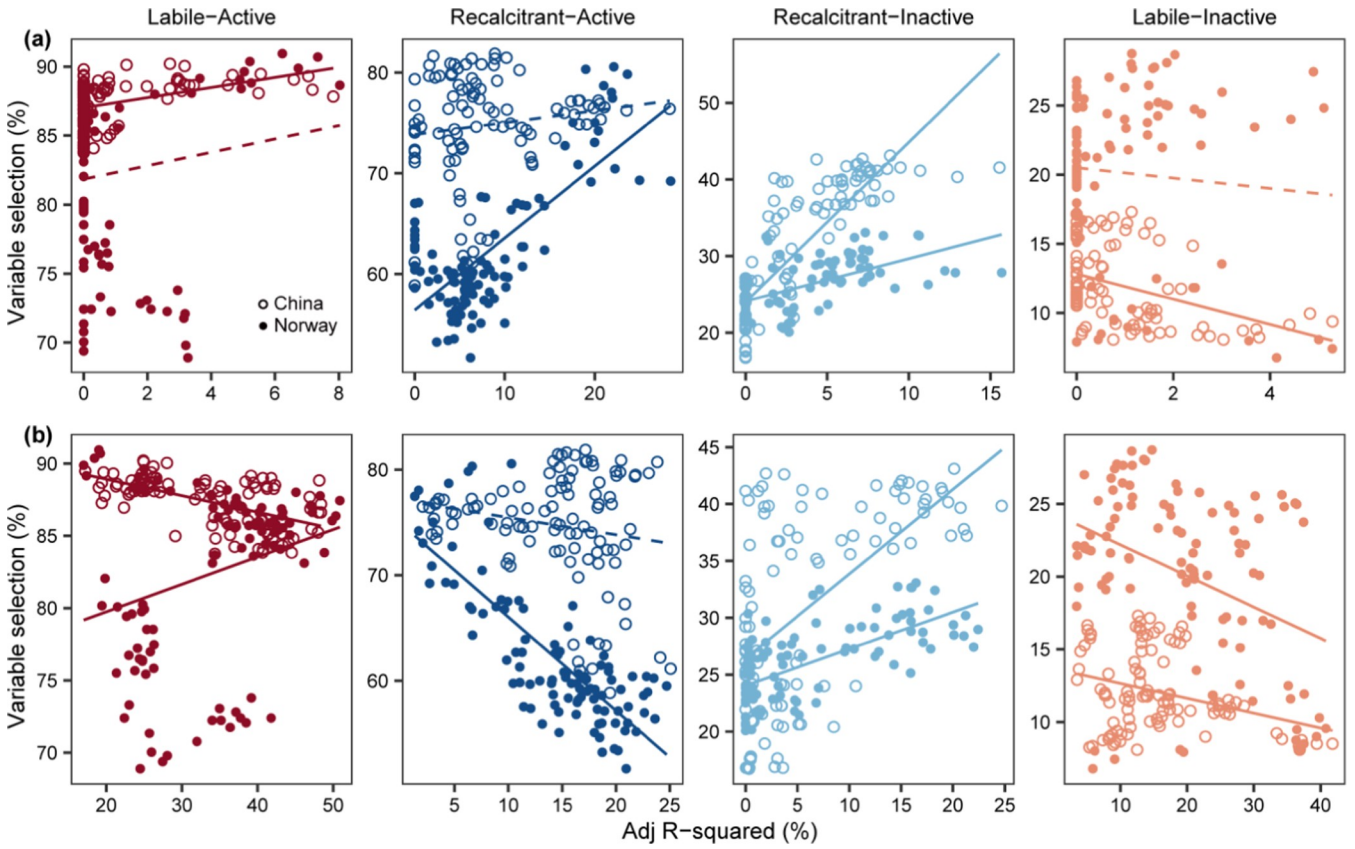

Figure 5. Relationships between variable selection and bacterial or environmental determinism underlying dissolved organic matter (DOM) fractions. For each DOM fraction, we fitted linear models between the relative importance of variable selection and the explained variations of bacterial communities (a) or environmental conditions (b) estimated from variable partitioning analysis along the energy supply (i.e., water pH) gradient in China (hollow points) and Norway (solid points). Solid and dotted lines indicate the statistically significant ($P \leq 0.05$) and nonsignificant ($P > 0.05$) relationships, respectively. Four DOM fractions are labile-active, recalcitrant-active, recalcitrant-inactive, and labile-inactive based on two dimensions of molecular reactivity and activity.

DOM assembly than systematic (i.e., deterministic) variation in the rates of production or transformation, which are likely to be low for the inactive fraction (Figure 3b).

Our data also suggest that the analogy between the Damköhler number and assembly processes is likely more complicated than the simple scenario discussed above. Within the inactive molecules, we observed stronger influences of deterministic processes in the recalcitrant fraction, relative to the labile fraction. We hypothesize that the recalcitrant-inactive fraction could persist longer than the labile-inactive fraction due to a combination of the inherent chemistry of recalcitrant molecules that slow their decomposition, and the emergent property of a lower number of putative biochemical transformations in the inactive molecules (Figure 3b). In turn, we hypothesize that the recalcitrant-inactive fraction may persist long enough so that its molecular composition becomes relative similar through space and time (Figure 3b). In this case, the rate of transport would have little influence over molecular composition even though the rates of production and transformation are putatively very low. Thus, molecules may enter the recalcitrant-inactive fraction deterministically (based on their chemistry) and then rarely leave (due to low transformation rates). This would result in the assembly of the recalcitrant-inactive fraction being deterministic, as observed here.

Variation in Assembly Processes under Global Change. To study further the potential drivers of variation in DOM assembly processes, we tested how the balance between stochastic and deterministic processes varied across the energy supply gradient for the four DOM fractions using a moving-window analysis. This analysis revealed that the relative influence of these processes varied along water pH gradients for both regions (Figures 3c, 4, S14, S16, and S17). For instance, the influence of variable selection changed with energy supply to a greater extent for the inactive than for active fraction, and this was true for both labile and recalcitrant molecules (Figure 3c). The connections between assembly processes and pH were stronger in Norway than in China except for the recalcitrant-inactive fraction (Figure 3c). More specifically, with elevated energy supply in both regions, the relative influence of variable selection was often increasingly dominant for active molecules, eventually reaching an asymptote (Figure 4). This finding is consistent with the strong divergence in DOM assemblages along pH gradients, especially for active fractions (Figure S18). The influence of variable selection also increased with energy supply for the recalcitrant-inactive fraction in both regions but decreased with and was a hump-shaped function of energy supply for the labile-inactive fraction in Norway and China, respectively (Figure 4). These results revealed that variable selection was more strongly connected to energy supply for inactive than for active molecules, irrespective of molecular reactivity (Figure 4).

https://doi.org/10.1021/acs.est.2c01432
Environ. Sci. Technol. 2022, 56, 10504−10516

Microbial versus Environmental Influences over DOM Composition. We further found that deterministic processes were generally associated with microbial effects and environmental filtering for each of the four fractions. For instance, in the active fractions, especially recalcitrant molecules, bacterial community composition was more important for structuring DOM composition as the relative importance of variable selection was positively correlated with the variation in DOM composition that was explained by bacterial community composition (Figure 5a) but generally negatively correlated with the variation that could be explained by environmental conditions (Figure 5b). In contrast, inactive fractions, especially recalcitrant molecules, were more influenced by environmental conditions than bacterial communities (Figure S19). However, the relative importance of variable selection still increased as more of the variation in DOM composition was explained by bacterial community composition in China (R^2 = 0.68, P < 0.001) and Norway (R^2 = 0.33, P < 0.001) (Figure 5a). These contrasting patterns of microbial and environmental influences across the four fractions varied along the energy supply gradients. Specifically, for active fractions, the bacterial effects were increasingly important toward higher water pH, in contrast to inactive fractions, wherein the influence of environmental conditions increased toward higher pH (Figure S19).

Collectively, our results indicate that, irrespective of the traditionally considered molecular bioavailability (i.e., lability vs recalcitrance),[9] the roles of bacterial and environmental influences were strong in structuring molecular composition for active and inactive fractions, respectively, especially at high productivity. The weaker bacterial influence on inactive fractions could be due to these compounds being less available to microbes caused by factors such as mineral protection and/or low concentrations of individual compounds.[64] These factors may lead to minimal microbial processing and, in turn, stochastic variation in which molecules are transformed.

Implications. The ecological processes structuring molecular assemblages of DOM remain challenging to discern, yet are critical for predicting the persistence of carbon under global change scenarios. Our study provides quantitative approaches to disentangle these ecological processes under any conditions of interest, such as global change, especially for contrasting DOM fractions that we characterized based on molecular reactivity and activity. No studies, to the best of our knowledge, have jointly considered these two important dimensions of DOM traits. Our results show that quantification of molecular activity could be a particularly useful way to identify the underlying mechanisms structuring DOM assemblages. Molecular activity may even be a better predictor of organic carbon persistence than the long-standing perception of recalcitrance[65] being an intrinsic property of organic molecules that determines their persistence.

Specifically, our results support this shift in focus from potential reactivity to realized activity, as the level of activity was the primary axis separating deterministic and stochastic assembly processes. That is, active and inactive fractions were primarily governed by deterministic and stochastic processes, respectively, across both labile and recalcitrant fractions. This phenomenon may be explained by our proposed hypotheses regarding the relative influences of deterministic production/transformation and stochastic transport, which is analogous to the Damköhler number and can conceptualize the dynamics of DOM compositional change (Figure 3b). Combining the DOMPart framework with other data, such as microbial gene expression and measured biogeochemical rates, can be used to further evaluate the inferences discussed above and reveal mechanisms controlling molecular activity. More broadly, this shift in focus toward realized activity is consistent with the shift away from focusing on intrinsic recalcitrance/lability in the carbon cycling literature of soil and marine ecosystems.[61,64,65]

We also found that within each level of molecular activity there were contrasting patterns in the ecological processes structuring labile versus recalcitrant molecules and their responses to global change. These results suggest that ecological processes could be better disentangled by including both dimensions of molecular reactivity and activity, rather than traditionally considering bulk DOM pools or reactivity pools alone.[8,58,66,67] Generally, our results and the DOMPart framework provide a new perspective on the processes structuring DOM by partitioning it into fractions based on multiple dimensions of molecular traits. Further application of the DOMPart framework across systems could ultimately be used to inform predictive ecosystem models, potentially at multiple scales from local scales to the Earth system. Collating DOMPart outcomes across systems could also provide data-driven predictions of the balance between stochastic and deterministic processes structuring DOM composition across environmental conditions and in response to global change.

Finally, our findings reveal that global change promotes an energy-dependent shift in the balance of stochastic and deterministic processes in structuring molecular assemblages of DOM. For active molecules, we documented that deterministic processes were increasingly important toward higher-energy supply, largely due to microbial processing. This finding should, in principle, make DOM compositional turnover more predictable in response to global change using molecular traits. However, we also found an increase in deterministic processes via environmental filtering and microbial processing in response to global change for inactive molecules and particularly the inactive recalcitrant fraction. This result was surprising because deterministic processes did not dominate the assembly of inactive molecules. Nonetheless, this result indicates that the molecular composition of inactive recalcitrant fraction may be increasingly predictable with increasing energy supply. The altered assembly processes in response to increased energy supply could be due to a variety of factors such as redox conditions leading to the release of DOM from reactive mineral surfaces[68] and thus elevating microbial activity, as indicated by the decreased molecular mass and increased N/C ratio (Figure S20). More generally, our results emphasize the need to consider both active and inactive fractions when predicting the fate of DOM. That is, the inactive DOM fractions accounted for 15−23% of all molecules across our samples (Table S3) and may provide a more stable carbon stock due to their low involvement in biogeochemical cycles. Our results collectively indicate that environmental change can substantially affect the compositional turnover of inactive fractions, with potential implications for biogeochemical functioning at ecosystem scales. Thus, the persistence of DOM in a changing world may largely rely on the sensitivity of these inactive fractions.

■ ASSOCIATED CONTENT

Supporting Information

The Supporting Information is available free of charge at https://pubs.acs.org/doi/10.1021/acs.est.2c01432.

https://doi.org/10.1021/acs.est.2c01432
Environ. Sci. Technol. 2022, 56, 10504−10516

Additional information on the methods of bacterial and DOM analyses, data on the relationships between energy supply and two global change drivers, distribution of molecular biochemical transformations of DOM, ecological processes for DOM molecules with different transformations, ecological processes underlying DOM assemblages with elevations or nutrient enrichment, drivers for βNTI, pH distribution, ecological processes underlying DOM assemblages with pH, relative abundance of DOM molecules, networks of DOM molecules, molecular traits of DOM, variability of ecological processes under global change, molecular composition of DOM, drivers for DOM composition, and molecular trait with pH (PDF)

AUTHOR INFORMATION

Corresponding Author

Jianjun Wang − *State Key Laboratory of Lake Science and Environment, Nanjing Institute of Geography and Limnology, Chinese Academic of Sciences, Nanjing 210008, China; University of Chinese Academy of Sciences, Beijing 100049, China;* orcid.org/0000-0001-7039-7136; Email: jjwang@niglas.ac.cn

Authors

Ang Hu − *College of Resources and Environment, Hunan Agricultural University, Changsha 410128, China; State Key Laboratory of Lake Science and Environment, Nanjing Institute of Geography and Limnology, Chinese Academic of Sciences, Nanjing 210008, China*

Kyoung-Soon Jang − *Bio-Chemical Analysis Team, Korea Basic Science Institute, Cheongju 28119, South Korea*

Fanfan Meng − *State Key Laboratory of Lake Science and Environment, Nanjing Institute of Geography and Limnology, Chinese Academic of Sciences, Nanjing 210008, China; University of Chinese Academy of Sciences, Beijing 100049, China*

James Stegen − *Pacific Northwest National Laboratory, Richland, Washington 99352, United States*

Andrew J. Tanentzap − *Ecosystems and Global Change Group, Department of Plant Sciences, University of Cambridge, Cambridge CB2 3EA, U.K.;* orcid.org/0000-0002-2883-1901

Mira Choi − *Bio-Chemical Analysis Team, Korea Basic Science Institute, Cheongju 28119, South Korea*

Jay T. Lennon − *Department of Biology, Indiana University, Bloomington, Indiana 47405, United States*

Janne Soininen − *Department of Geosciences and Geography, University of Helsinki, Helsinki, FIN 00014, Finland*

Complete contact information is available at: https://pubs.acs.org/10.1021/acs.est.2c01432

Author Contributions

◆A.H., K.-S.J., and F.M. contributed equally to this paper. J.W. conceived the idea. J.W. carried out the field trips and provided the physicochemical and biological data. M.C. and K.-S.J. analyzed the DOM. F.M. performed the statistical analyses with the comments from A.H. and J.W. A.H. wrote the first draft of the manuscript. A.H. and J.W. finished the manuscript with the comments from K.-S.J., J. Stegen., A.J.T., J.T.L., and J. Soininen. All authors contributed to the intellectual development of this study.

Notes

The authors declare no competing financial interest.

The scripts in FT-ICR-MS data analysis are publicly available at https://github.com/danczakre/Meta-Metabolome_Ecology and in the R package iDOM at http://github.com/jianjunwang/iDOM. Environmental and bacterial community data are reported in Wang et al. (2016). Other data are available from the corresponding author upon reasonable request.

ACKNOWLEDGMENTS

The authors appreciate Lizhou Dai, Chengyan Zhang, Jinfu Liu, Yongqiang Zhou, and Feiyan Pan for field sampling and lab analyses, Ji Shen, Qinglong Wu, Yongqin Liu, Shaoda Liu, Xiancai Lu, and Yahai Lu for kind support and comments, and Yunlin Zhang and Thorsten Dittmar for key introductions. This study was supported by the National Natural Science Foundation of China (91851117, 42077052, and 41871048) and the CAS Key Research Program of Frontier Sciences (QYZDB-SSW-DQC043). K.-S.J. was supported by the National Research Foundation of Korea (NRF) funded by the Ministry of Science and ICT (MSIT) (NRF-2021M1A5A1075510) and KBSI (C140440) grants. J.C.S. was supported by a U.S. Department of Energy (U.S. DOE) Early Career Award (grant 74193) at Pacific Northwest National Laboratory, a multiprogram national laboratory operated by Battelle for the U.S. DOE under contract no. DE-AC05−76RL01830. A.J.T. was supported by a H2020 ERC Grant (sEEIngDOM 804673). J.T.L. was supported by the National Science Foundation (DEB-1934554), the U.S. Army Research Office Grant (W911NF-14-1-0411), and the National Aeronautics and Space Administration (80NSSC20K0618).

REFERENCES

(1) Graham, E. B.; Crump, A. R.; Kennedy, D. W.; Arntzen, E.; Fansler, S.; Purvine, S. O.; Nicora, C. D.; Nelson, W.; Tfaily, M. M.; Stegen, J. C. Multi 'omics comparison reveals metabolome biochemistry, not microbiome composition or gene expression, corresponds to elevated biogeochemical function in the hyporheic zone. *Sci. Total Environ.* **2018**, *642*, 742−753.

(2) Stegen, J. C.; Johnson, T.; Fredrickson, J. K.; Wilkins, M. J.; Konopka, A. E.; Nelson, W. C.; Arntzen, E. V.; Chrisler, W. B.; Chu, R. K.; Fansler, S. J.; Graham, E. B.; Kennedy, D. W.; Resch, C. T.; Tfaily, M.; Zachara, J. Influences of organic carbon speciation on hyporheic corridor biogeochemistry and microbial ecology. *Nat. Commun.* **2018**, *9*, No. 585.

(3) Tanentzap, A. J.; Fitch, A.; Orland, C.; Emilson, E. J. S.; Yakimovich, K. M.; Osterholz, H.; Dittmar, T. Chemical and microbial diversity covary in fresh water to influence ecosystem functioning. *Proc. Natl. Acad. Sci. U.S.A.* **2019**, *116*, 24689.

(4) Zhang, C.; Dang, H.; Azam, F.; Benner, R.; Legendre, L.; Passow, U.; Polimene, L.; Robinson, C.; Suttle, C. A.; Jiao, N. Evolving paradigms in biological carbon cycling in the ocean. *Natl. Sci. Rev.* **2018**, *5*, 481−499.

(5) Catalá, T. S.; Reche, I.; Fuentes-Lema, A.; Romera-Castillo, C.; Nieto-Cid, M.; Ortega-Retuerta, E.; Calvo, E.; Álvarez, M.; Marrasé, C.; Stedmon, C. A.; Álvarez-Salgado, X. A. Turnover time of fluorescent dissolved organic matter in the dark global ocean. *Nat. Commun.* **2015**, *6*, No. 5986.

(6) Jiao, N.; Herndl, G. J.; Hansell, D. A.; Benner, R.; Kattner, G.; Wilhelm, S. W.; Kirchman, D. L.; Weinbauer, M. G.; Luo, T.; Chen, F.; Azam, F. Microbial production of recalcitrant dissolved organic matter: long-term carbon storage in the global ocean. *Nat. Rev. Microbiol.* **2010**, *8*, 593−599.

(7) Lugato, E.; Lavallee, J. M.; Haddix, M. L.; Panagos, P.; Cotrufo, M. F. Different climate sensitivity of particulate and mineral-associated soil organic matter. *Nat. Geosci.* **2021**, *14*, 295−300.
(8) Fang, C.; Smith, P.; Moncrieff, J. B.; Smith, J. U. Similar response of labile and resistant soil organic matter pools to changes in temperature. *Nature* **2005**, *433*, 57−59.
(9) Qin, S.; Chen, L.; Fang, K.; Zhang, Q.; Wang, J.; Liu, F.; Yu, J.; Yang, Y. Temperature sensitivity of SOM decomposition governed by aggregate protection and microbial communities. *Sci. Adv.* **2019**, *5*, No. eaau1218.
(10) Davidson, E. A.; Janssens, I. A. Temperature sensitivity of soil carbon decomposition and feedbacks to climate change. *Nature* **2006**, *440*, 165−173.
(11) Reich, P. B.; Hobbie, S. E.; Lee, T. D.; Rich, R.; Pastore, M. A.; Worm, K. Synergistic effects of four climate change drivers on terrestrial carbon cycling. *Nat. Geosci.* **2020**, *13*, 787−793.
(12) Koch, B. P.; Dittmar, T. From mass to structure: an aromaticity index for high-resolution mass data of natural organic matter. *Rapid Commun. Mass Spectrom.* **2006**, *20*, 926−932.
(13) Janssens, I. A.; Dieleman, W.; Luyssaert, S.; Subke, J. A.; Reichstein, M.; Ceulemans, R.; Ciais, P.; Dolman, A. J.; Grace, J.; Matteucci, G.; Papale, D.; Piao, S. L.; Schulze, E. D.; Tang, J.; Law, B. E. Reduction of forest soil respiration in response to nitrogen deposition. *Nat. Geosci.* **2010**, *3*, 315−322.
(14) Mau, R. L.; Liu, C. M.; Aziz, M.; Schwartz, E.; Dijkstra, P.; Marks, J. C.; Price, L. B.; Keim, P.; Hungate, B. A. Linking soil bacterial biodiversity and soil carbon stability. *ISME J.* **2015**, *9*, 1477−1480.
(15) Roth, V.-N.; Lange, M.; Simon, C.; Hertkorn, N.; Bucher, S.; Goodall, T.; Griffiths, R. I.; Mellado-Vázquez, P. G.; Mommer, L.; Oram, N. J.; Weigelt, A.; Dittmar, T.; Gleixner, G. Persistence of dissolved organic matter explained by molecular changes during its passage through soil. *Nat. Geosci.* **2019**, *12*, 755−761.
(16) Marschner, B.; Kalbitz, K. Controls of bioavailability and biodegradability of dissolved organic matter in soils. *Geoderma* **2003**, *113*, 211−235.
(17) Kellerman, A. M.; Kothawala, D. N.; Dittmar, T.; Tranvik, L. J. Persistence of dissolved organic matter in lakes related to its molecular characteristics. *Nat. Geosci.* **2015**, *8*, 454−457.
(18) Graham, E. B.; Tfaily, M. M.; Crump, A. R.; Goldman, A. E.; Bramer, L. M.; Arntzen, E.; Romero, E.; Resch, C. T.; Kennedy, D. W.; Stegen, J. C. Carbon Inputs From Riparian Vegetation Limit Oxidation of Physically Bound Organic Carbon Via Biochemical and Thermodynamic Processes. *J. Geophys. Res.: Biogeosci.* **2017**, *122*, 3188−3205.
(19) Moran, M. A.; Kujawinski, E. B.; Stubbins, A.; Fatland, R.; Aluwihare, L. I.; Buchan, A.; Crump, B. C.; Dorrestein, P. C.; Dyhrman, S. T.; Hess, N. J.; Howe, B.; Longnecker, K.; Medeiros, P. M.; Niggemann, J.; Obernosterer, I.; Repeta, D. J.; Waldbauer, J. R. Deciphering ocean carbon in a changing world. *Proc. Natl. Acad. Sci. U.S.A.* **2016**, *113*, 3143−3151.
(20) Danczak, R. E.; Chu, R. K.; Fansler, S. J.; Goldman, A. E.; Graham, E. B.; Tfaily, M. M.; Toyoda, J.; Stegen, J. C. Using metacommunity ecology to understand environmental metabolomes. *Nat. Commun.* **2020**, *11*, No. 6369.
(21) Chase, J. M. Ecological niche theory. *Theory Ecol.* **2011**, 93−107.
(22) Stegen, J. C.; Lin, X.; Fredrickson, J. K.; Konopka, A. E. Estimating and mapping ecological processes influencing microbial community assembly. *Front. Microbiol.* **2015**, *6*, 370.
(23) Hubbell, S. P. *The Unified Neutral Theory of Biodiversity and Biogeography (MPB-32)*; Princeton University Press, 2011.
(24) Wang, J.; Pan, F.; Soininen, J.; Heino, J.; Shen, J. Nutrient enrichment modifies temperature-biodiversity relationships in large-scale field experiments. *Nat. Commun.* **2016**, *7*, No. 13960.
(25) Hu, A.; Choi, M.; Tanentzap, A. J.; Liu, J.; Jang, K.-S.; Lennon, J. T.; Liu, Y.; Soininen, J.; Lu, X.; Zhang, Y.; Shen, J.; Wang, J. Ecological networks of dissolved organic matter and microorganisms under global change. *Nat. Commun.* **2022**, DOI: 10.1038/s41467-41022-31251-41461.
(26) Lauro, F. M.; McDougald, D.; Thomas, T.; Williams, T. J.; Egan, S.; Rice, S.; DeMaere, M. Z.; Ting, L.; Ertan, H.; Johnson, J.; Ferriera, S.; Lapidus, A.; Anderson, I.; Kyrpides, N.; Munk, A. C.; Detter, C.; Han, C. S.; Brown, M. V.; Robb, F. T.; Kjelleberg, S.; Cavicchioli, R. The genomic basis of trophic strategy in marine bacteria. *Proc. Natl. Acad. Sci. U.S.A.* **2009**, *106*, 15527−15533.
(27) Livermore, J. A.; Emrich, S. J.; Tan, J.; Jones, S. E. Freshwater bacterial lifestyles inferred from comparative genomics. *Environ. Microbiol.* **2014**, *16*, 746−758.
(28) Newton, R. J.; Griffin, L.; Loftis, K.; Meile, C.; Gifford, S.; Givens, C.; Howard, E.; King, E.; Oakley, C.; Reisch, C.; Rinta-Kanto, J.; Sharma, S.; Sun, S.; Varaljay, V.; Vila-Costa, M.; Westrich, J.; Moran, M. A. Genome characteristics of a generalist marine bacterial lineage. *ISME J.* **2010**, *4*, 784−798.
(29) Li, H.; Yang, S.; Semenov, M. V.; Yao, F.; Ye, J.; Bu, R.; Ma, R.; Lin, J.; Kurganova, I.; Wang, X.; Deng, Y.; Kravchenko, I.; Jiang, Y.; Kuzyakov, Y. Temperature sensitivity of SOM decomposition is linked with a K-selected microbial community. *Global Change Biol.* **2021**, *27*, 2763−2779.
(30) Giardina, C. P.; Ryan, M. G. Evidence that decomposition rates of organic carbon in mineral soil do not vary with temperature. *Nature* **2000**, *404*, 858−861.
(31) Wang, J.; Hu, A.; Meng, F.; Zhao, W.; Yang, Y.; Soininen, J.; Shen, J.; Zhou, J. Embracing mountain microbiome and ecosystem functions under global change. *New Phytol.* **2022**, *234*, 1987−2002.
(32) Caporaso, J. G.; Kuczynski, J.; Stombaugh, J.; Bittinger, K.; Bushman, F. D.; Costello, E. K.; Fierer, N.; Pena, A. G.; Goodrich, J. K.; Gordon, J. I.; Huttley, G. A.; Kelley, S. T.; Knights, D.; Koenig, J. E.; Ley, R. E.; Lozupone, C. A.; McDonald, D.; Muegge, B. D.; Pirrung, M.; Reeder, J.; Sevinsky, J. R.; Tumbaugh, P. J.; Walters, W. A.; Widmann, J.; Yatsunenko, T.; Zaneveld, J.; Knight, R. QIIME allows analysis of high-throughput community sequencing data. *Nat. Methods* **2010**, *7*, 335−336.
(33) Choi, J. H.; Jang, E.; Yoon, Y. J.; Park, J. Y.; Kim, T. W.; Becagli, S.; Caiazzo, L.; Cappelletti, D.; Krejci, R.; Eleftheriadis, K.; Park, K. T.; Jang, K. S. Influence of Biogenic Organics on the Chemical Composition of Arctic Aerosols. *Global Biogeochem. Cycles* **2019**, *33*, 1238−1250.
(34) Dittmar, T.; Koch, B.; Hertkorn, N.; Kattner, G. A simple and efficient method for the solid-phase extraction of dissolved organic matter (SPE-DOM) from seawater. *Limnol. Oceanogr. Methods* **2008**, *6*, 230−235.
(35) Tolić, N.; Liu, Y.; Liyu, A.; Shen, Y.; Tfaily, M. M.; Kujawinski, E. B.; Longnecker, K.; Kuo, L.-J.; Robinson, E. W.; Paša-Tolić, L.; Hess, N. J. Formularity: Software for Automated Formula Assignment of Natural and Other Organic Matter from Ultrahigh-Resolution Mass Spectra. *Anal. Chem.* **2017**, *89*, 12659−12665.
(36) Kujawinski, E. B.; Behn, M. D. Automated Analysis of Electrospray Ionization Fourier Transform Ion Cyclotron Resonance Mass Spectra of Natural Organic Matter. *Anal. Chem.* **2006**, *78*, 4363−4373.
(37) Kim, S.; Kramer, R. W.; Hatcher, P. G. Graphical Method for Analysis of Ultrahigh-Resolution Broadband Mass Spectra of Natural Organic Matter, the Van Krevelen Diagram. *Anal. Chem.* **2003**, *75*, 5336−5344.
(38) Koch, B. P.; Dittmar, T. From mass to structure: an aromaticity index for high-resolution mass data of natural organic matter. *Rapid Commun. Mass Spectrom.* **2016**, *30*, 250.
(39) LaRowe, D. E.; Van Cappellen, P. Degradation of natural organic matter: A thermodynamic analysis. *Geochim. Cosmochim. Acta* **2011**, *75*, 2030−2042.
(40) Hughey, C. A.; Hendrickson, C. L.; Rodgers, R. P.; Marshall, A. G.; Qian, K. Kendrick Mass Defect Spectrum: A Compact Visual Analysis for Ultrahigh-Resolution Broadband Mass Spectra. *Anal. Chem.* **2001**, *73*, 4676−4681.
(41) Song, H.-S.; Stegen, J. C.; Graham, E. B.; Lee, J.-Y.; Garayburu-Caruso, V. A.; Nelson, W. C.; Chen, X.; Moulton, J. D.; Scheibe, T. D.

Representing Organic Matter Thermodynamics in Biogeochemical Reactions via Substrate-Explicit Modeling. *Front. Microbiol.* **2020**, *11*, No. 531756.
(42) Schneidman-Duhovny, D.; Bramer, L. M.; White, A. M.; Stratton, K. G.; Thompson, A. M.; Claborne, D.; Hofmockel, K.; McCue, L. A. ftmsRanalysis: An R package for exploratory data analysis and interactive visualization of FT-MS data. *PLoS Comput. Biol.* **2020**, *16*, No. e1007654.
(43) Lavorel, S.; Grigulis, K.; McIntyre, S.; Williams, N. S. G.; Garden, D.; Dorrough, J.; Berman, S.; Quétier, F.; Thébault, A.; Bonis, A. Assessing functional diversity in the field − methodology matters! *Funct. Ecol.* **2007**, *22*, 134−147.
(44) Breitling, R.; Ritchie, S.; Goodenowe, D.; Stewart, M. L.; Barrett, M. P. Ab initio prediction of metabolic networks using Fourier transform mass spectrometry data. *Metabolomics* **2006**, *2*, 155−164.
(45) Friedman, J.; Alm, E. J. Inferring Correlation Networks from Genomic Survey Data. *PLoS Comput. Biol.* **2012**, *8*, No. e1002687.
(46) Kurtz, Z. D.; Müller, C. L.; Miraldi, E. R.; Littman, D. R.; Blaser, M. J.; Bonneau, R. A. Sparse and Compositionally Robust Inference of Microbial Ecological Networks. *PLoS Comput. Biol.* **2015**, *11*, No. e1004226.
(47) Proulx, S. R.; Promislow, D. E.; Phillips, P. C. Network thinking in ecology and evolution. *Trends Ecol. Evol.* **2005**, *20*, 345−353.
(48) D'Andrilli, J.; Cooper, W. T.; Foreman, C. M.; Marshall, A. G. An ultrahigh-resolution mass spectrometry index to estimate natural organic matter lability. *Rapid Commun. Mass Spectrom.* **2015**, *29*, 2385−2401.
(49) Swenson, N. G.; Anglada-Cordero, P.; Barone, J. A. Deterministic tropical tree community turnover: evidence from patterns of functional beta diversity along an elevational gradient. *Proc. R. Soc. B* **2011**, *278*, 877−884.
(50) Swenson, N. G.; Stegen, J. C.; Davies, S. J.; Erickson, D. L.; Forero-Montaña, J.; Hurlbert, A. H.; Kress, W. J.; Thompson, J.; Uriarte, M.; Wright, S. J.; Zimmerman, J. K. Temporal turnover in the composition of tropical tree communities: functional determinism and phylogenetic stochasticity. *Ecology* **2012**, *93*, 490−499.
(51) Ning, D.; Yuan, M.; Wu, L.; Zhang, Y.; Guo, X.; Zhou, X.; Yang, Y.; Arkin, A. P.; Firestone, M. K.; Zhou, J. A quantitative framework reveals ecological drivers of grassland microbial community assembly in response to warming. *Nat. Commun.* **2020**, *11*, No. 4717.
(52) Stegen, J. C.; Lin, X.; Konopka, A. E.; Fredrickson, J. K. Stochastic and deterministic assembly processes in subsurface microbial communities. *ISME J.* **2012**, *6*, 1653−1664.
(53) Wang, J.; Shen, J.; Wu, Y.; Tu, C.; Soininen, J.; Stegen, J. C.; He, J.; Liu, X.; Zhang, L.; Zhang, E. Phylogenetic beta diversity in bacterial assemblages across ecosystems: deterministic versus stochastic processes. *ISME J.* **2013**, *7*, 1310−1321.
(54) Oksanen, J.; Blanchet, F. G.; Kindt, R.; Legendre, P.; Minchin, P.; O'Hara, R. B.; Simpson, G.; Solymos, P.; Stevens, M. H. H.; Wagner, H. *vegan: Community Ecology Package. CRAN R package*, 2017.
(55) Miller, J. K.; Farr, S. D. Bimultivariate redundancy: a comprehensive measure of interbattery relationship. *Multivar. Behav. Res.* **1971**, *6*, 313−324.
(56) Felipe-Lucia, M. R.; Soliveres, S.; Penone, C.; Fischer, M.; Ammer, C.; Boch, S.; Boeddinghaus, R. S.; Bonkowski, M.; Buscot, F.; Fiore-Donno, A. M.; Frank, K.; Goldmann, K.; Gossner, M. M.; Hölzel, N.; Jochum, M.; Kandeler, E.; Klaus, V. H.; Kleinebecker, T.; Leimer, S.; Manning, P.; Oelmann, Y.; Saiz, H.; Schall, P.; Schloter, M.; Schöning, I.; Schrumpf, M.; Solly, E. F.; Stempfhuber, B.; Weisser, W. W.; Wilcke, W.; Wubet, T.; Allan, E. Land-use intensity alters networks between biodiversity, ecosystem functions, and services. *Proc. Natl. Acad. Sci. U.S.A.* **2020**, *117*, 28140−28149.
(57) Carlson, M. L.; Flagstad, L. A.; Gillet, F.; Mitchell, E. A. D. Community development along a proglacial chronosequence: are above-ground and below-ground community structure controlled more by biotic than abiotic factors? *J. Ecol.* **2010**, *98*, 1084−1095.
(58) Craine, J. M.; Fierer, N.; McLauchlan, K. K. Widespread coupling between the rate and temperature sensitivity of organic matter decay. *Nat. Geosci.* **2010**, *3*, 854−857.
(59) Hansell, D. A. Recalcitrant dissolved organic carbon fractions. *Annu. Rev. Mar. Sci.* **2013**, *5*, 421−445.
(60) Zakem, E. J.; Cael, B. B.; Levine, N. M. A unified theory for organic matter accumulation. *Proc. Natl. Acad. Sci. U.S.A.* **2021**, *118*, No. e2016896118.
(61) Kothawala, D. N.; Kellerman, A. M.; Catalan, N.; Tranvik, L. J. Organic Matter Degradation across Ecosystem Boundaries: The Need for a Unified Conceptualization. *Trends Ecol. Evol.* **2021**, *36*, 113−122.
(62) Li, L.; Sullivan, P. L.; Benettin, P.; Cirpka, O. A.; Bishop, K.; Brantley, S. L.; Knapp, J. L. A.; van Meerveld, I.; Rinaldo, A.; Seibert, J.; Wen, H.; Kirchner, J. W. Toward catchment hydro-biogeochemical theories. *Wiley Interdiscip. Rev.: Water* **2021**, *8*, No. e1495.
(63) Maher, K. The role of fluid residence time and topographic scales in determining chemical fluxes from landscapes. *Earth Planet. Sci. Lett.* **2011**, *312*, 48−58.
(64) Schmidt, M. W. I.; Torn, M. S.; Abiven, S.; Dittmar, T.; Guggenberger, G.; Janssens, I. A.; Kleber, M.; Kogel-Knabner, I.; Lehmann, J.; Manning, D. A.; Nannipieri, P.; Rasse, D. P.; Weiner, S.; Trumbore, S. E. Persistence of soil organic matter as an ecosystem property. *Nature* **2011**, *478*, 49−56.
(65) Dittmar, T.; Lennartz, S. T.; Buck-Wiese, H.; Hansell, D. A.; Santinelli, C.; Vanni, C.; Blasius, B.; Hehemann, J.-H. Enigmatic persistence of dissolved organic matter in the ocean. *Nat. Rev. Earth Environ.* **2021**, *2*, 570−583.
(66) Wieder, W. R.; Allison, S. D.; Davidson, E. A.; Georgiou, K.; Hararuk, O.; He, Y.; Hopkins, F.; Luo, Y.; Smith, M. J.; Sulman, B.; Todd-Brown, K.; Wang, Y.-P.; Xia, J.; Xu, X. Explicitly representing soil microbial processes in Earth system models. *Global Biogeochem. Cycles* **2015**, *29*, 1782−1800.
(67) Rofner, C.; Peter, H.; Catalán, N.; Drewes, F.; Sommaruga, R.; Pérez, M. T. Climate-related changes of soil characteristics affect bacterial community composition and function of high altitude and latitude lakes. *Global Change Biol.* **2017**, *23*, 2331−2344.
(68) Faust, J. C.; Tessin, A.; Fisher, B. J.; Zindorf, M.; Papadaki, S.; Hendry, K. R.; Doyle, K. A.; Marz, C. Millennial scale persistence of organic carbon bound to iron in Arctic marine sediments. *Nat. Commun.* **2021**, *12*, No. 275.

https://doi.org/10.1021/acs.est.2c01432
Environ. Sci. Technol. 2022, 56, 10504−10516